Kinetics and Catalysis, Vol. 42, No. 3, 2001, pp. 381–389. Translated from Kinetika i Kataliz, Vol. 42, No. 3, 2001, pp. 422–431.

IV RUSSIAN CONFERENCE WITH THE PARTICIPATION OF CIS COUNTRIES ON THE SCIENTIFIC BASES OF CATALYST PREPARATION AND TECHNOLOGY

New Trends in the Development of Methods for Catalyst Preparation for the Processes of Organochlorine Synthesis

I. I. Kurlyandskaya*, I. G. Solomonik, E. D. Glazunova*, Yu. A. Treger*, and M. R. Flid***

** State Unitary Enterprise SINTEZ, Scientific Research Institute and Design Office, Moscow, Russia*

*** Zelinskii Institute of Organic Chemistry, Russian Academy of Sciences, Moscow, 119992 Russia*

Received September 18, 2000

Abstract—The formation of heterogeneous mercury-, zinc-, and copper-containing catalytic systems obtained by supporting salt components (SCs) without a solvent is studied. It is shown that due to strong interaction between SC and support, the size of salt clusters on the surface and their relative contribution decrease. That is, the concentration of excess salt phases decreases. The dispersity increases up to molecular distribution. When surface-linked two-dimensional disordered structures are formed, the state of salt phases in the compositions of catalytic systems changes. The surface mobility of salt clusters during the contact with the reaction medium is found. Compared to the systems obtained by impregnation with aqueous solutions, the proposed systems are 2–3 times more thermally stable, their surface is enriched in defect structures that are active in catalysis, and the processes of organochlorine synthesis become more efficient.

INTRODUCTION

The future of industrial organochlorine synthesis is associated with the creation of highly active, selective, and stable catalysts. Conventional quasiadsorption and impregnation methods for the preparation of supported salt catalysts ($CuCl_2$–Al_2O_3, $ZnCl_2$–Al_2O_3, and $HgCl_2$–active carbon) are based on the impregnation of support by the aqueous solutions of active salt components (SC) under static conditions or under the conditions of vigorous stirring of supports and solutions with further drying.

These methods have several shortcomings from the standpoint of formation of optimal catalysts: SC hydrolysis, the hydration of the developed surface of a support, and a change in the initial localization of SCs due to the capillary carry-over of the solution and the formation of coarsely-dispersed phases during drying.

The formation of multicomponent heterophase salt catalytic systems based on copper, zinc, and mercury chlorides on different supports is carried out along the following three main lines [1–5]: (a) the formation of bulk near-surface phases with different degrees of order due to the intercalation of metal ions into vacant octahedral and tetrahedral sites of a support (alumina) lattice or into the interplane spaces of graphite-like crystal lattice of the carbon support (activated carbon); the immobilization of SCs on different active sites of support surface and the formation of linked two-dimensional nonstoichiometric disordered structures; and (c) the growth of islands of isolated surface three-dimensional clusters of excess SCs or the products of its hydrolysis and thermolysis followed by agglomeration. It depends on the methods and conditions for catalyst preparation which of the system states would dominate and which of them would determine its activity and stability.

Salt catalytic systems obtained under mild conditions by supporting dissolved SCs are at an unsteady state. They are capable of relaxation in the reaction medium at the temperatures of catalysis, and this relaxation may result in a decrease in the activity and stability [6, 7].

We develop new procedure for the catalyst preparation based on radically different methods for supporting SCs:

– spraying of an SC solution into a fluidized bed of support together with fast simultaneous drying ensures uniform supporting of salt (the method of supporting into fluidized bed, SFB);

– adsorption of salt with a high vapor pressure from the gas phase by support (the method of dry thermal treatment, DTT); and

– direct contacting of SCs and support in the presence of a solvent in the discrete isothermal mode (the DTT method).

We expect that, under these conditions, the interaction between SC and support will intensively occur even at 150–250°C because the developed surface of the boundary between two phases, which are at the state of phase transitions, is highly reactive in topochemical reactions (according to the Headwall principle [8, 9]). The formation of catalytic systems is possible where SC is at different, more active and stable states.

0023-1584/01/4203-0381$25.00

The goal of this work is to study the processes of formation of supported salt catalysts on supports with different chemical natures in the absence of a solvent and to study the relations between catalyst genesis and their performance characteristics.

EXPERIMENTAL

The samples of model catalytic systems were studied, including $HgCl_2$, $ZnCl_2$, KCl–$ZnCl_2$, $CuCl_2$, and KCl–$CuCl_2$ on different supports. Henceforth, these samples are denoted by first symbols of chemical formulas and the phase composition of the support. For instance, CuAl(γ) denotes the $CuCl_2$–γ-Al_2O_3 system.

$HgCl_2$–activated carbon (HgAC). Samples prepared according to the DTT method by adsorption of $HgCl_2$ vapors on AGN-2 active carbon contained 10 and 20 wt % of $HgCl_2$ (10HgAC and 20HgAC). The sample obtained by impregnation by an aqueous $HgCl_2$ solution using a standard technique with further drying at 110°C had 10 wt % $HgCl_2$. The specific surface area S_{sp} of AGN-2 active carbon was 840 m^2/g.

$ZnCl_2$–Al_2O_3 (ZnAl(γ)). Samples with 14 wt % Zn were prepared by both the standard impregnation of AOA-1 alumina (S_{sp} = 190 m^2/g) by an aqueous solution of $ZnCl_2$ or by the equimolar mixture of KCl and $ZnCl_2$ with further drying at 150°C and using the DTT method. According to XPS, the support was γ-Al_2O_3 with some insignificant admixture of pseudoboehmite [5].

$CuCl_2$–Al_2O_3 (CuAl). Samples with 4–5 wt % Cu were prepared by the standard impregnation of α-Al_2O_3 (S_{sp} = 10 m^2/g) or γ-Al_2O_3 (S_{sp} = 120 m^2/g, IKT-02-6M from AO Katalizator) by an aqueous solution of $CuCl_2$ (or the equimolar mixture of KCl and $CuCl_2$) with further drying at 150°C, as well as using the DTT and SFB methods.

Alumina contained admixtures of different phases according to XPS.

To compare with the CuAl samples, we used the commercial MEDC catalyst from Süd–Chemie–MT, which contained 4% Cu.

The diffraction patterns of polycrystalline samples were recorded using a Dron-2 instrument (CuK_α irradiation; Ni filter). Reflexes were identified using data reported in [10]. Several diffraction patterns were obtained using an UVD-2000 high-temperature X-ray chamber. The samples were heated from 20 to 500°C.

To obtain the small-angle X-ray scattering (SAXS) spectra, a KRM-1 chamber was used (CuK_α irradiation; Ni filter). The intensity was measured at scattering angles of 6–600′. To exclude interference effects due to the coincidence of scattering centers (support pores and SC in them), the pores of support were filled with glycerol. The indicator functions of scattering were found using the method described in [11].

To determine the electron states of copper ions and their coordination to the surface, we used diffuse-reflectance electron spectroscopy. MgO was used as a reflectance standard. Spectra were registered using a Hitachi-330 spectrophotometer with an integrating sphere and a Shimadzu MPS 50L spectrophotometer equipped with an attachment for recording reflectance spectra in the regime of the optical density relative to air.

Topochemical and phase transformations in the near-surface layer with a thickness of the Debye radius of charge shielding (10–100 nm) was studied by the method of thermal vacuum electric conductivity by measuring the direct current conductivity (σ) of the sample in a vacuum at a stepwise increase in temperature and the activation energy of conductivity (E_σ) [12].

SC desorption was determined under dynamic conditions using neutron-activated analysis. For that catalyst grains were irradiated by a neutron flow of 3×10^{13} cm^{-2} s^{-1} in a reactor. The activity was measured using an IN-96B γ-spectrometer.

HCl adsorption was measured using a vacuum setup with samples treated beforehand in a vacuum [5]. The distribution of surface regions over probe HCl molecule adsorption heats was calculated from the experimental adsorption isotherm at iterations. The contribution from clean surface was taken into account [5, 8].

Prepared catalysts were tested in the following processes:

– Copper-containing catalysts were tested in the oxidative chlorination of ethylene (in an integral fluidized-bed reactor, T = 220°C, C_2H_4 : HCl : O_2 = 1.07 : 2 : 0.7);

– Zinc-containing catalysts were tested in the reaction of methanol with HCl (in an integral fluidized-bed reactor, T = 250°C, CH_3OH : HCl = 1 : 1.25); and

– Mercury-containing catalysts were tested in acetylene hydrochlorination (in a differential reactor with a vibrofluidized bed, T = 180°C, C_2H_2 : HCl = 1 : 1.3).

RESULTS AND DISCUSSION

HgAC. Figure 1 shows the fragments of diffraction patterns of some samples (2θ = 10–30°). Reflexes belonging to $HgCl_2$ were not seen even in the case of 20HgAC (the maximum at 2θ = 26.7° belongs to α-quartz admixed in active carbon). Therefore, the salt phase on the surface of active carbon is X-ray amorphous (disordered) or highly dispersed. At 2θ angles ranging from 20 to 30°, all diffraction patterns has a diffuse maximum, which can be interpreted as a (002) reflex corresponding to the interplanar distance d(002) between lengthy graphite-like lattices [13]. The calculated values of d(002) equal to 0.367 nm for active carbon and 0.375 nm for 10HgAC, are close. For the 20HgAC, the maximum corresponds to d(002) = 0.414 nm. An increase in the interlayer distances in the catalyst samples points to the localization of $HgCl_2$ in the graphite-like lattice with the formation of an intercalation compound [14].

As follows from SAXS data, described as a dependence of the logarithm of the scattered light intensity on the logarithm of scattering angles φ (φ changes from 6

to 600′), the difference in the scattering intensity over the 10HgAC sample and over the support is small despite substantial difference in the electron densities of $HgCl_2$ and active carbon (Fig. 2). The intensity of scattering over $HgCl_2$ in the HgAC system is approximately half the intensity of scattering over active carbon. On the other hand, the intensity of platinum scattering in the PtAC systems is twice as high as scattering of supported platinum, whereas platinum exists on the surface in the form of 0.4–2.0-nm clusters [15]. Provided that sizes of particles of the active phase in both systems are about the same, comparison of these data for two systems suggest that $HgCl_2$ mostly exists on the surface in the molecularly dispersed state, and the amount of agglomerated $HgCl_2$ is 10–15% on the surface.

Figure 3 shows the normalized curves of the volume distribution of active phase particles over inertia radii (R_i) (the latter characterize the distribution of the scattering substance relative to the center of gravity of a specific particle). These data suggest that the sizes of salt agglomerates and their relative volume primarily depend on the method of supporting. As calculation using the spherical-cluster model shows, each cluster may include up to one hundred $HgCl_2$ molecules. The 10HgAC sample obtained by the DTT method (Fig. 3, curve *1*) is the most dispersed. Comparison of relative cluster volumes proportional to their weights (relative volumes are determined using the areas under the distribution curves in Fig. 3) shows that the weight portion of clusters in the latter case is approximately half that in the sample obtained by impregnation (the relative volumes are 510 and 930, respectively). The cluster radius corresponding to the maximum on the distribution curve and the average cluster radius in the DTT sample is lower than in the sample obtained by impregnation (Fig. 3, curves *1* and *3*).

Under the reaction conditions, clusters become mobile. This is reflected in a change in the distribution of clusters over sizes. The maximum on curves shifts toward higher R_i values; that is, the size of clusters increases (Fig. 3, curves *2* and *4*). At the same time, the weight fraction of clusters decreases because of $HgCl_2$ thermal desorption in the reaction medium. Thus, the relative volume of clusters in the DTT sample decreases from 510 to 400, and the relative volume of clusters in the samples prepared by impregnation decreases from 930 to 630. The dispersity of the salt phase probably directly affects this process. This hypothesis agrees with the fact that the rate of $HgCl_2$ desorption from the highly dispersed sample decreases from 0.22 to 0.8% per hour.

Thus, during the reaction in the catalytic system, salt clusters grow simultaneously with salt phase desorption from the surface. Experiments showed that the loss of salt phase due to desorption is greater than the amount of initially aggregated salt. The removal of the salt component from small surface clusters is more dif-

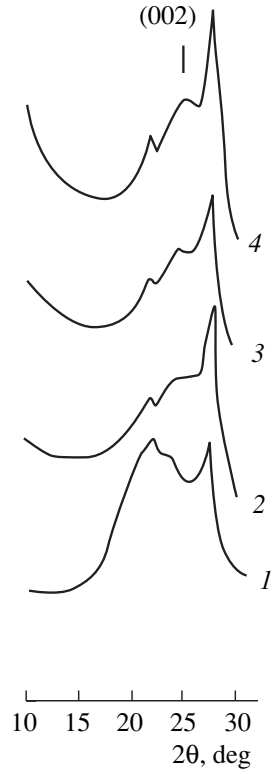

Fig. 1. Fragments of the diffraction patterns of support and catalysts: (*1*) 20HgAC (DTT), (*2*) 10HgAC (impregnation), (*3*) 10HgAC (DTT), and (*4*) active carbon support.

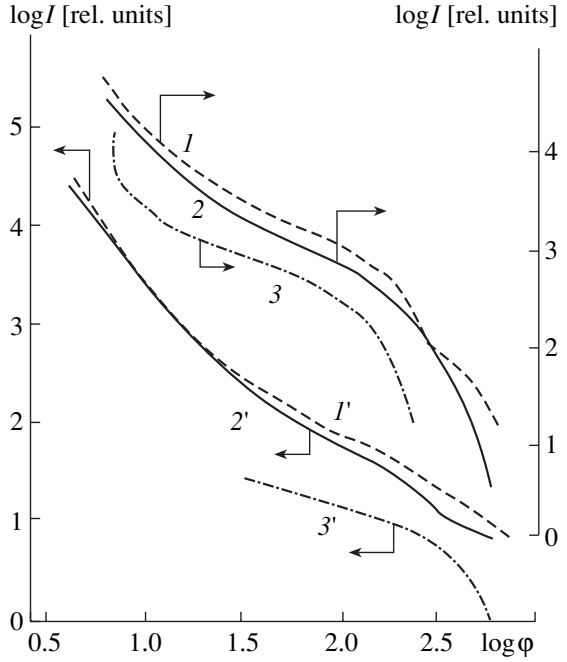

Fig. 2. Intensity *I* of small-angle X-ray scattering on different samples: (*1*, *1*') 10HgAC (impregnation), (*2*, *2*') active carbon support, (*3*, *3*' the salt component of the catalyst $HgCl_2$; (*1*', *2*', *3*') samples with pores filled with glycerol.

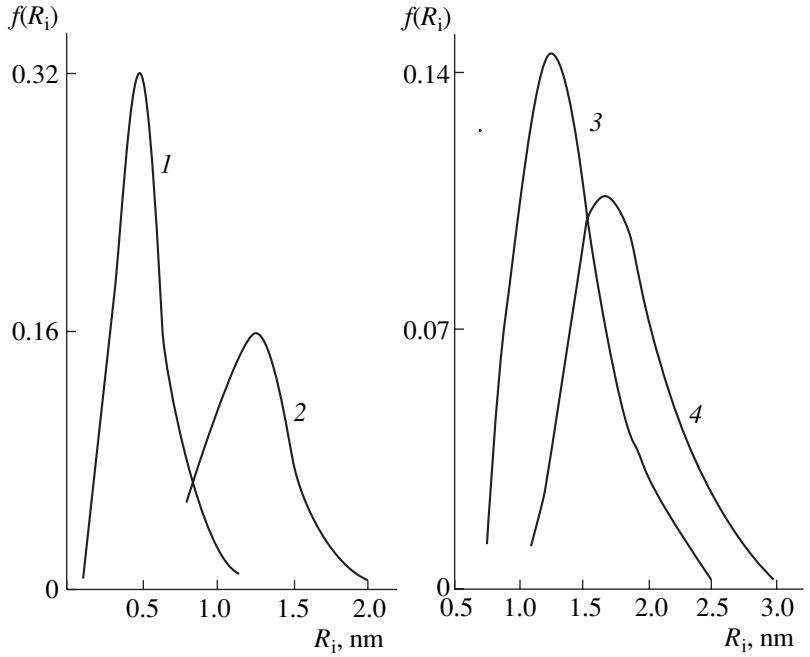

Fig. 3. Distribution of the volumes of $HgCl_2$ salt clusters over sizes: (*1*, *3*) 10HgAC catalysts prepared by the DTT method and impregnation, respectively; (*2*, *4*) the same catalysts after working in the reaction medium.

ficult than the removal from large mercuric chloride clusters (that is, $HgCl_2$ desorbs from large aggregates). Therefore, we conclude that, during the reaction, the coalescence of small clusters and their replenishment by molecularly dispersed phase compensate for the loss of large clusters [16].

A decrease in the fraction of salt clusters as the dispersity of the salt phase increases up to the molecular distribution results in the stabilization of the catalytic HgAC system. The catalyst prepared by the DTT method, unlike the catalyst prepared by impregnation, does not change its activity for a long time in acetylene hydrochlorination. On the DTT sample, the conversion remains constant (80%) for 100 h. On the sample obtained by impregnation the conversion decreases to 40%.

ZnAl(γ). When the solvent is heated in a high-temperature X-ray chamber at 300–400°C, the pseudoboehmite lines disappear from the diffraction pattern because of the pseudoboehmite $\longrightarrow$ γ-Al_2O_3 phase transition [5]. After supporting the salt component onto Al_2O_3 by impregnation (the XPS phase composition includes $ZnCl_2$, $ZnO \cdot ZnCl_2 \cdot 2H_2O$, $ZnCl_2 \cdot 1.33H_2O$, and $4ZnO \cdot ZnCl_2 \cdot 4H_2O$), a diffraction pattern appears that has a nonadditive nature: it does not contain reflexes from the $ZnCl_2$ phase and reflexes from hydroxychlorides are weak. This pattern points to significant disorder of zinc-containing excess phases on the support surface.

Further heating of the sample from 200 to 500°C results in the disappearance of reflexes from hydroxychlorides and in an increase in the intensity of reflexes at 2θ 31.2–36.8°. These correspond to the formation of a solid solution when Zn^{2+} occupies vacant tetrahedral positions of γ-Al_2O_3. Similar structures cover 5 to 20 layers [17].

When SCs are supported by the DTT method with heating to 300°C, the activity of pseudoboehmite phases increases near the phase-transition point (the Headwall effect). Simultaneously, the state of zinc-containing phases changes due to dehydration and dehydroxylation, and this change is favorable for the more active interaction of zinc-containing phases with metastable phases of support. The diffraction patterns of the sample heated in the high-temperature X-ray chamber at 100– 500°C point to a successive increase in the intensity of reflexes from zinc–aluminum spinel. The latter is formed as a result of solid Zn^{2+}–Al_2O_3 solution transition into the phase of nonstoichiometric spinel.

In the diffuse-reflectance electronic spectra of zinc-containing systems, we observed bands at 268, 360, and 520 nm (Fig. 4, curves *2–4*), and the spectrum of $ZnCl_2$ dehydrated in a flow of HCl contains a narrow absorption band at 255 nm and bands at 360 and 520 nm (Fig. 4, curve *1*).

These bands cannot be assigned to either Zn^{2+} (d^{10}) or Zn^+, which is characterized by bands near 300 nm [18]. However, in the visible region of the spectrum, the sample had a color characteristic of nonstoichiometric zinc oxide, which has an acceptor level at 2.5 eV in the forbidden zone. This level refers to transition between zinc vacancy and the conduction band $V^-_{Zn} \longleftrightarrow V^0_{Zn} + \bar{e}$ [19].

According to [20], the negatively charged zinc vacancy V_{Zn} in ZnS and ZnSe has optical transitions with 2.65 and 1.4 eV, and such vacancies are stable at room temperature. Thus, the band at 520 nm corresponding to the energy of optical transition equal to 2.4 eV can be assigned to a cationic vacancy, which appears during the process of proper $ZnCl_2$ disordering.

The bands at 255, 268, and 360 nm are in the region of charge-transfer bands. Comparison of curves *2* and *4* suggests that the intensities of these bands increase with an increase in the degree of salt–support interaction. According to [21], the structure of zinc chloride and zinc–potassium chloride systems (crystalline and amorphous) can be described as a set of structures obtained by a combination of elementary $ZnCl_4$ cells bound to each other in a specific manner, wherein each cell has a certain contribution. The fact that the intensities of absorption bands at 268 and 360 nm change similarly and the high values of these intensities, which are not typical of the DTT method, suggest that these are largely charge-transfer bands that can be assigned to the structures whose concentration increases with an increase in the degree of amorphism and in the dispersion of the excessive salt component.

Proceeding from the structure of the salt component [21], the charge-transfer band at 268 nm should be assigned to a charge-transfer complex that involves an oxygen-containing fragment and the zinc ion in the isolated tetrahedron. The band at 360 nm should be assigned to a charge-transfer complex with zinc ions in associated tetrahedrons. The bands at 255 and 360 nm observed in the spectrum of the model sample of zinc chloride are probably due to charge transfer from structural hydroxyls to specially coordinated zinc ions.

Our data are suggestive of the formation of zinc chloride catalytic systems with charge transfer. These systems involve surface hydroxyls or lattice oxygen as ligands. An increase in the intensity of the corresponding adsorption bands in the ZnAl(γ) system obtained by the DTT method (Fig. 4, curve *2*) is due to strengthened SC–support interaction.

The above findings allow us to explain the behavior of zinc-containing catalysts, which work in methyl chloride synthesis from methanol and HCl for a long time. An increase in the stability of the ZnAl(γ) catalyst obtained by the DTT method while preserving high conversion (the conversion of methanol was 98–99%) is due to a decrease in the SC desorption rate and the absence of salt phases (from 0.06 to 0.02% per hour) and to the formation of surface solid solutions and linked surface structures that are active in catalysis

CuAl. Comparison of thermal vacuum electric conductivity (TVEC) curves (Fig. 5) points to a substantial difference between model KCuAl(α) systems obtained by impregnation and the DTT method (curves *1* and *4*). Curve *1*, which describes the dependence of the activation energy E_σ of conductivity on the temperature of evacuation T_{evac}, is stipulated by the presence of several

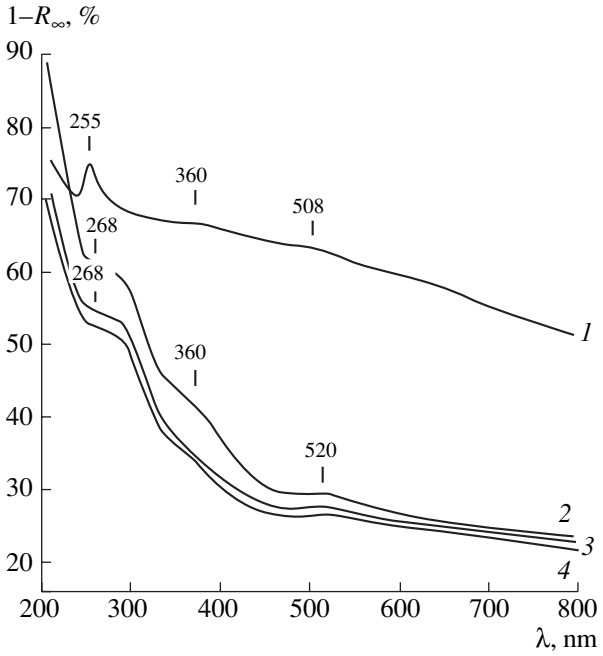

Fig. 4. Diffuse-reflectance electron spectra of the model and catalytic systems: (*1*) $ZnCl_2$ treated with HCl; (*2*) ZnAl(γ) prepared by the DTT method; (*3*) ZnKAl(γ) prepared by impregnation; and (*4*) ZnAl(γ) prepared by impregnation.

phases that are formed when KCl and $CuCl_2$ are supported on the surface of contacting particles by impregnation. The analogous DTT system (curve *4*) is characterized by the presence of two branches on the curve. The existence of a high-energy branch points to the segregation of the salt system on the surface and to the presence of disordered phases close to those formed in the KCl–$KCuCl_3$ system. Analysis of TVEC curves [22] shows that, at low T_{evac}, SCs are distributed over the surface in the form of island, but heating to 200°C (the Huttig temperature of surface mobility for $CuCl_2$) is favorable for the interaction between SCs supported on different adsorption sites. In this case, the corresponding phases and structures are formed of which a decrease in E_σ with an increase in T_{evac} is characteristic. Because pre-melting processes may occur at 350°C in the CuCl–$CuCl_2$ system, which appears in the process of KCl–$CuCl_2$ segregation and which forms an eutectic mixture with a melting point of 380°C [9], the appearance of the low-temperature branch of E_σ can reasonably be associated with the existence of this surface phase.

In the model KCuAl(γ) system, the $CuCl_2$ phase (curves *2* and *3*) exists separately from KCl up to T_{evac} = 150°C. With an increase in T_{evac}, a portion of $CuCl_2$ is thermolyzed to form an X-ray amorphous phase with many defects. This is reflected in the appearance of low-energy branches of curves *2* and *3*. Another portion of $CuCl_2$ reacts with KCl and produces the KCl–$KCuCl_3$ system to which the high-energy branch of curve *2* belongs. The difference in the behavior of

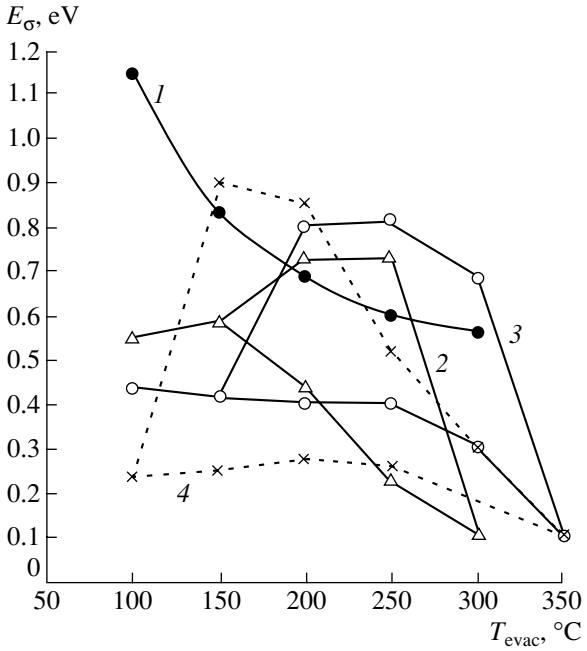

Fig. 5. Curves of thermal vacuum electric conductivity for the model catalytic systems: (*1*) KCuAl(α) prepared by impregnation; (*2*) KCuAl(γ) prepared by impregnation; (*3*) KCuAl(α) prepared by the DTT method; and (*4*) KCuAl(γ) prepared by the DTT method.

systems obtained by impregnation (curve *2*) and the DTT method (curve *3*) (the value of E_σ decreases to the value at 300°C rather than 350°C) points to the different states of SCs in these cases. In the case of a sample prepared by impregnation, the KCl–$KCuCl_3$ system (m.p. 280°C [1]) is formed. In the case of the DTT method, the KCl–K_2CuCl_4 system (m.p. 320–330°C [1]) is formed. The absence of melting effects on derivatograms of KCuAl(γ) [9] means that SCs at the premelting state react with the support and forms surface solid solutions and linked surface structures with the closest order. These are characterized by a low value of E_σ by analogy with KCu melts on silica gels [22].

Analysis of the diffuse-reflectance electron spectra of the model systems under study (Fig. 6) points to the existence of some relation between the method of SC supporting and the state of copper ions. In the KCuAl(γ) system, considerable portion of copper ions is distributed independently of KCl over octahedral vacancies of the support. This is reflected in the absorption bands at 810 and 830 nm in the region of *d–d* transitions of Cu^{2+}_{Oh}, which differ from the bands of the salt component and KCuAl(α) catalysts [23]. The salt component that does not enter the lattice bulk contains the Cu^{2+}_{Th} ion (an absorption band at 950 nm and a shoulder at 340 nm). This ion enters the composition of structures linked to the support surface, which are close to those available in the KCl–$CuCl_2$ system. However, the main portion of copper is distributed over the surface either in the form of isolated ions with a charge transfer band at 265 nm (which is due to the charge transfer from the chlorine ligand to Cu^{2+} or in the form of Cu^{2+}–X–Cu^{2+} associates characterized by a charge-transfer band at 365 nm.

As follows from the spectra with low concentrations of the active component, Cu^{2+} ions exist on the developed surface in octahedral and tetrahedral positions of the support lattice and in tetrahedral structures that probably appear when SC is linked via anionic hydroxyl group exchange for chlorine from the coordination sphere of Cu^{2+}.

The spectrum of the KCuAl(α) system contains the bands reflecting different states of copper ions. The charge-transfer band at 365 nm points to the presence of associated Cu^{2+} ions on the surface. A charge-transfer band at 510 nm is due to the presence of copper ions in the chain structure of excess $KCuCl_3$. If a sample is prepared by the DTT method using a temperature higher than usual temperature of drying after impregnation, then all absorption bands become more intense in the KCuAl(α) system. This points to an increase in the number of chromophores and to the dispersing of SC. The centroid of the *d–d* transition $^2E_g \longrightarrow {}^2T_{2g}$ band shifts to 810–830 nm, which is characteristic of Cu^{2+} in the octahedral vacancies of γ-Al_2O_3.

In the KCuAl(α) system prepared by the DTT method, the intensity of absorption bands in the region of *d–d* transitions is higher than in an analogous system prepared by impregnation. In the region of charge-transfer bands, the disappearance or shift of a number of bands is observed: the band at 265 nm, which is characteristic of isolated Cu^{2+} ions shifts to 262 nm; the intensity at 340 nm decreases; and the band at 365 nm from associated copper ions becomes a shoulder. Apparent changes in the spectra point to strengthened interactions between the copper-containing component and support, which results in the partial transfer of associated and isolated Cu^{2+} cations to the support lattice and in an increase in the concentration of linked surface copper-containing structures.

Diffraction patterns obtained in the study of real copper-containing catalysts, based on microspherical IKT-02-6M support, for the oxidative chlorination of ethylene (Fig. 7, curves *2* and *3*) were different depending on the preparation procedure (impregnation or DTT). The support contained the phase of γ-Al_2O_3 with an admixed θ-Al_2O_3 phase. Relative concentrations of γ- and θ phases can be estimated from the relative intensities of the bands $2\theta = 44.9°$ ($d = 0.021$ nm) for the θ phase and $2\theta = 45.9°$ ($d = 0.1977$ nm) for the γ phase [10]. The upper estimate of the γ-Al_2O_3 phase concentration is 70%. The CuAl(γ) catalyst prepared by impregnation contained different copper-containing phases which were formed during the interaction of support surface groups with copper chloride. In addition to $Cu_2(OH)_3Cl$, which is usually present, we detected the $Cu(OH,Cl) \cdot 2H_2O$ hydrate and

the products of support surface chlorination, e.g. $AlCl_3 \cdot 4Al(OH)_3 \cdot 4H_2O$. The formation of these compounds can be explained by the chemical corrosion of incompletely crystallized γ-Al_2O_3. Several lines in the diffraction pattern from the support of the catalyst are better resolved than in the diffraction pattern of the support because they are superposed with lines from the defect spinel solid solutions of copper in the latter case.

It is known that the selective formation of bulk $Cu_2(OH)_3Cl$ occurs during impregnation of γ-Al_2O_3, which has a basic surface, by an aqueous solution of salt. This support probably contains basic hydroxyls on the surface, but the diffraction pattern of the dried catalyst does not contain reflexes that are characteristic of CuO. This points to not very high basicity of these centers. The formation of CuO is stipulated by the formation of $Cu(OH)_2$ during the exchange of the Cl^- ion with very basic OH group on the surface and further decomposition of copper hydroxide to copper oxide during catalyst drying (the maximum of hydration peak at 144°C) [9].

Depending on the preparation procedure of the CuAl(γ) catalyst, different states of SCs are formed in all copper-containing structures in the composition of this catalyst. These include the states that are formed during bulk interaction with the support lattice, the states linked to the surface, and excess SC. For both preparation procedures, considerable X-ray amorphism of SCs is typical. However, in the case of DTT samples, copper-containing complex anions form anionic copper–chlorine sublattices with structures in which order/disorder transition occurs in the temperature range close to that for the salt systems K_2CuCl_4 and $KCuCl_3$ (despite the absence of KCl in the system) [2].

Due to the participation of anionic surface hydroxyls in the formation of anionic hydroxychlorides highly dispersed β-$Cu_2(OH)_3Cl$ is formed instead of the α phase. In general, when the catalyst is prepared by the DTT method, more active interaction between the support and SCs are observed. The salt system is dispersed and becomes X-ray amorphous. The surface is enriched in the linked and bulk disordered phases of aluminates.

The diffraction pattern of the known commercial MEDC catalyst for the oxidative chlorination of ethylene (curve *4*) also contains the lines of disordered aluminates. Although the salt component is at the highly dispersed state, we observed weak reflexes from $CuCl_2$ phases and hydroxychlorides like $Cu_2(OH)_3Cl$ and $CuCl_2 \cdot 3[Cu(OH)_2]$. We also observed reflexes corresponding to d equal to 0.729, 0.429, 0.363, and 0.273 nm, which point to the presence of disordered multiple surface layers of SC with structures of anionic chlorine–copper sublattice close to the K_2CuCl_4 and $KCuCl_3$ phases.

Thus, the DTT method makes it possible to obtain the catalyst with a surface structure close to that of the MEDC catalyst. This is only possible when the SC–support surface interaction is strong. The presence of different copper containing phases is responsible for the energetic nonuniformity of the catalyst surface with different adsorption sites.

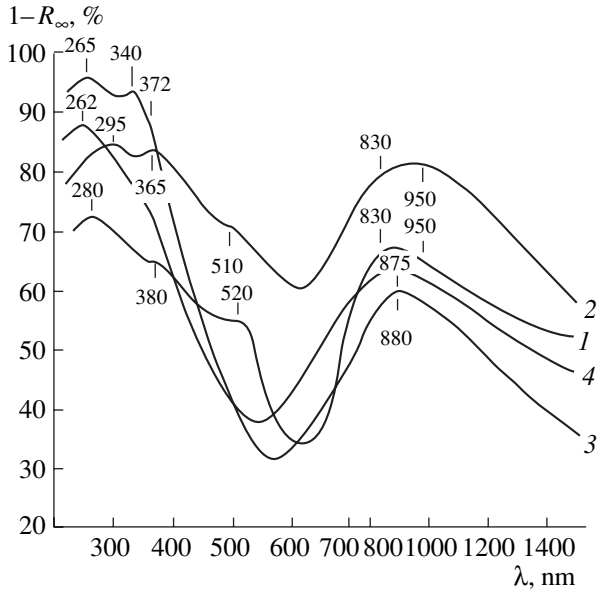

Fig. 6. Diffuse-reflectance electron spectra of the catalytic systems treated thermally at 250°C: (*1*) KCuAl(α) prepared by impregnation; (*2*) KCuAl(α) prepared by the DTT method; (*3*) KCuAl(γ) prepared by impregnation; and (*4*) KCuAl(γ) prepared by the DTT method.

Figure 8 shows the distribution of catalyst surface regions over the heats of adsorption of probe HCl. According to [5], the peaks of adsorption heats correspond to the spectrum of the states of nonuniform surface. Highly dispersed intercalation structures like copper aluminates and different surface-linked and excess disordered states of copper-containing salt phases with close but different structures are present on the catalyst surfaces. This is reflected in the discreteness of adsorption heats. The MEDC catalyst and the CuAl(γ) catalyst prepared by the DTT method differ from the CuAl(γ) sample prepared by impregnation: the contribution of peaks corresponding to intercalation structures (Q > 90 kJ/mol) and defect, surface-linked copper-containing phases with the anionic sublattices close to sublattices of $KCuCl_3$ and K_2CuCl_4 (Q = 60–70 kJ/mol) is much more pronounced.

For the distribution curve of the heat of HCl adsorption on the catalyst prepared by impregnation, the largest peak is in the region of Q = 70–80 kJ/mol. This peak reflects the interaction of HCl with excess (bulk) surface salt phases characterized by X-ray diffraction.

Thus, for the formation of catalytic copper-containing salt systems (as well as zinc- and mercury-containing systems described above) some general regularities are seen, but the DTT method maintains the localization of active salt component supported on the surface

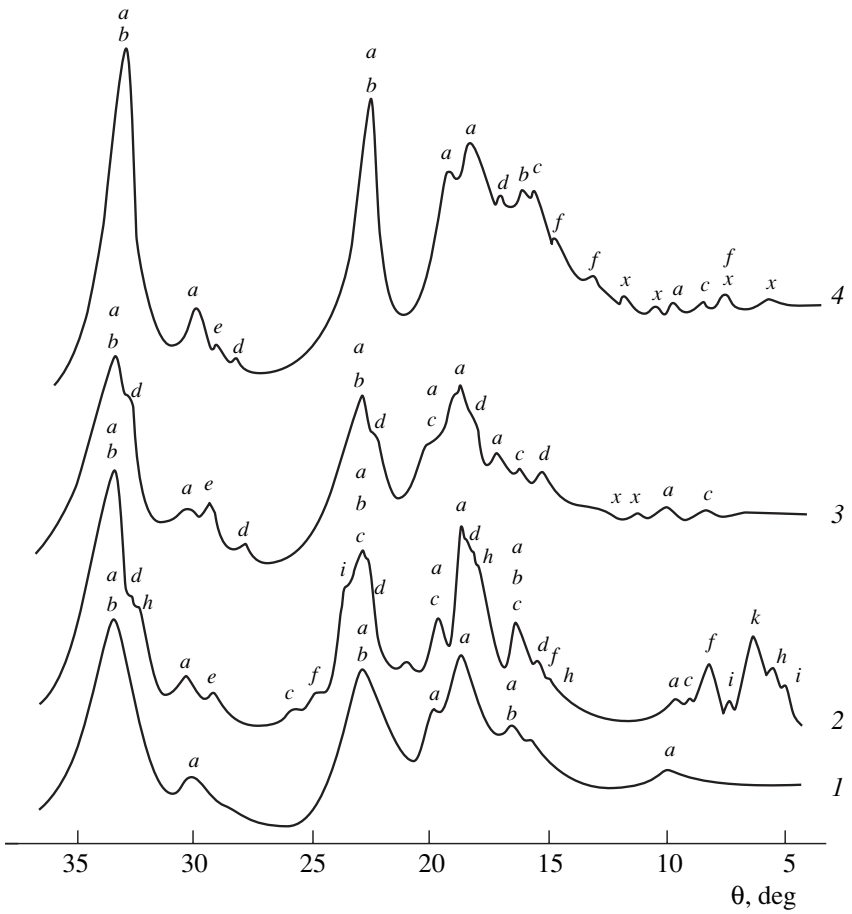

Fig. 7. Diffraction patterns of the support and different samples of copper-containing catalysts: (*1*) IKT-02-6M support; (*2*) CuAl(γ) prepared by impregnation; (*3*) CuAl(γ) prepared by the DTT method; (*4*) MEDC. Notation: (*a*) γ-Al_2O_3, (*b*) θ-Al_2O_3, (*c*) $Cu_2(OH)_3Cl$, (*d*) $CuAl_2O_4$, (*e*) β-$CuAlO_2$, (*f*) $CuCl_2$, (*h*) $Al_{11}(OH)_{30}Cl$, (*i*) $AlCl_3 \cdot 4Al(OH)_3 \cdot 4H_2O$, (*k*) Cu(OH,Cl) · $2H_2O$, (*x*) K_2CuCl_4 or $KCuCl_3$-like phase.

that favors the formation of linked defect structures with perturbed long-range order and highly dispersed intercalation structures due to the strengthened interaction between SCs and support.

The presence of the above states of copper-containing phases predetermines high performance characteristics of a catalyst prepared by the DTT method in the process of the oxidative chlorination of ethylene. The catalysts prepared by DTT or SFB methods show better characteristics in this process under standard conditions than the catalyst prepared by impregnation. Specifically, their fluidized bed is more homogeneous, and the selectivity to dichloroethane is higher (the average concentration of 1,2-dichloroethane in the product is 0.2–0.3% higher than in the case of a traditional sample prepared by impregnation when oxygen is used as an oxidant). The efficiency of ethylene conversion at 215–220°C on these catalysts reaches 96% and approaches the efficiency of the MEDC catalyst. We also found that the process can be carried out on these catalysts under the conditions that model the "oxygen regime" (the oxidant is oxygen).

Thus, the catalysts prepared by the DTT and SFB methods on IKT-02-6M support are better than the catalyst prepared by impregnation. However, to create a catalytic system which is not worse than the MEDC catalyst, further improvement of the support is needed.

Our experimental study allowed us to find that the formation of catalytic systems in the absence of a solvent (the DTT method) is determined by a high reactivity of the boundaries between disordered solid phases in topochemical reactions. As a result of stronger (than in the case of conventional impregnation) interaction between SC and support, the sizes and fraction of salt clusters on the surface decrease. That is, the amount of excess salt phases decreases and the dispersity of SC approaches the molecular level. The state of salt phases in the catalyst composition changes. Because of this, the thermal stability of the catalysts increases by a factor of 2–3, and their surfaces are enriched in linked and bulk defect structures, which are active in catalysis. This is favorable for an increase in the activity and selectivity of the catalytic systems in the process of

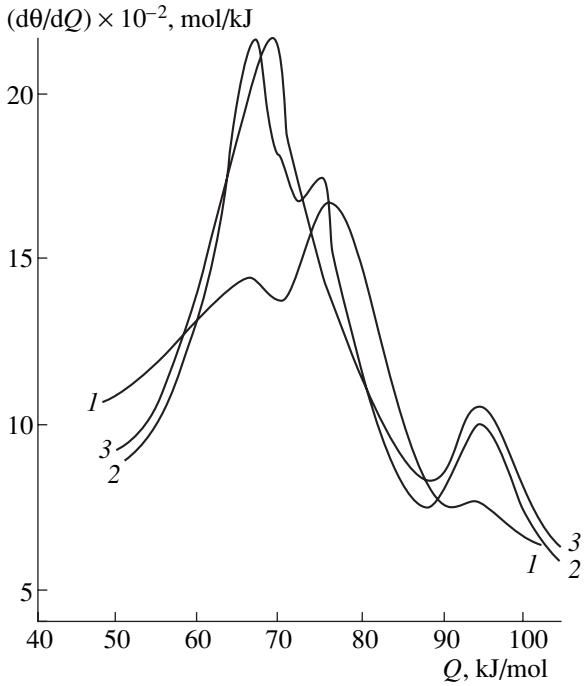

Fig. 8. Distribution of surface regions of copper-containing catalysts over the heats of HCl adsorption: (*1*) CuAl(γ) prepared by impregnation; (*2*) CuAl(γ) prepared by the DTT method; and (*3*) MEDC.

organochlorine synthesis. When contacting with the reaction medium, salt clusters show surface mobility.

Based on this study, we developed new technologies for catalyst preparation.

REFERENCES

1. Solomonik, I.G., Kurlyandskaya, I.I., Danyushevsky, V.Ya., and Jakerson, V.I., *Supplement to Proc. 8th Int. Conf. on Thermal Analysis*, Bratislava, 1985, p. 37.
2. Solomonik, I.G., Kurlyandskaya, I.I., Ashavskaya, G.A., and Yakerson, V.I., *Izv. Akad. Nauk SSSR, Ser. Khim.*, 1986, no. 4, p. 766.
3. Glazunova, E.D., Kurlyandskaya, I.I., Boevskaya, E.A., *et al.*, *Kinet. Katal.*, 1987, vol. 28, no. 5, p. 1178.
4. Glazunova, E.D., Kurlyandskaya, I.I., Boevskaya, E.A., *et al.*, *Kinet. Katal.*, 1987, vol. 28, no. 5, p. 1183.
5. Kurlyandskaya, I.I., Dashevskii, M.I., Solomonik, I.G., *et al.*, *Izv. Akad. Nauk SSSR, Ser. Khim.*, 1987, no. 6, p. 1220.
6. Kurlyandskaya, I.I., Solomonik, I.G., Glazunova, E.D., and Yakerson, V.I., *Tez. dokl. III Vsesoyuz. konf. "Nestatsionarnye protsessy v katalize"* (Abstracts of papers, III All-Union Conf. on Nonstationary Processes in Catalysis), Novosibirsk, 1986, part 2, p. 97.
7. Flid, M.R., Kurlyandskaya, I.I., Solomonik, I.G., and Babotina, M.V., *Khim. Prom-st.*, 1996, no. 6, p. 34.
8. Jaycock, M.J. and Parfitt, G.D., *Chemistry of Interfaces*, Chichester: Wiley, 1984, pp. 146, 179.
9. Solomonik, I.G., Kurlyandskaya, I.I., Danyushevskii, V.Ya., and Yakerson, V.I., *Izv. Akad. Nauk SSSR, Ser. Khim.*, 1984, no. 10, p. 2180.
10. *X-Ray PDF, Data Cards, Inorganic Section, JCPDS*, 1948–1984.
11. Plavnik, G.M., *Kristallografiya*, 1984, vol. 29, no. 2, p. 210.
12. Dulov, A.A. and Abramova, L.A., *Itogi Nauki Tekh., Ser. Kinet. Katal.*, 1984, vol. 12, p. 144.
13. Semikolenov, V.A., *Usp. Khim.*, 1992, vol. 61, no. 2, p. 320.
14. Behrens, P., Alidoosti, M., Schutz, Z., *et al.*, *Z. Naturforsch. B*, 1989, vol. 44b, p. 721.
15. Plavnik, G.M., Parlits, B.P., and Dubinin, M.M., *Dokl. Akad. Nauk SSSR*, 1972, vol. 206, no. 2, p. 399.
16. Selivanov, V.N., Plavnik, G.M., Glazunova, E.D., *et al.*, *Izv. Akad. Nauk SSSR, Ser. Khim.*, 1989, no. 11, p. 2420.
17. Strohmeier, B. and Hercules, D., *J. Catal.*, 1984, vol. 86, no. 2, p. 266.
18. Buxton, G.V. and Sellers, R.M., *J. Chem. Soc., Faraday Trans. I*, 1975, vol. 71, no. 3, p. 558.
19. Boccuzi, F., Ghiotti, G., and Chiorino, A., *J. Chem. Soc., Faraday Trans. II*, 1983, vol. 79, no. 12, p. 1779.
20. Emtsev, V.V. and Mashkovets, T.V., *Primesi i tochechnye defekty v poluprovodnikakh* (Impurities and Point Defects in Semiconductors), Moscow: Radio i Svyaz', 1981, pp. 26, 40.
21. Takagi, Y. and Nakamuro, T., *J. Chem. Soc., Faraday Trans. I*, 1985, vol. 81, no. 8, p. 1901.
22. Solomonik, I.G., Dulov, A.A., Abramova, L.A., *et al.*, *Tez. dokl. I Vsesoyuz. konf. "Kataliz i kataliticheskie protsessy proizvodstva khim.-farm. preparatov"* (Abstracts of Papers, I All-Union Conf. on Catalysis and Catalytic Processes in Pharmaceutics), Moscow, 1985, part. 1, p. 76.
23. Solomonik, I.G., Kurlyandskaya, I.I., and Yakerson, V.I., *Tez. dokl. II Vseros. nauch. soveshchaniya "Vysokoorganizovannye kataliticheskie sistemy"* (Abstracts of Papers, II All-Russian Conf. on Highly Organized Catalytic Systems), Moscow, 2000, p. 31.